Structural Engineering and Mechanics, *Vol. 49, No. 3 (2014) 395-410*
DOI: http://dx.doi.org/10.12989/sem.2014.49.3.395

Horizontal stiffness solutions for unbonded fiber reinforced elastomeric bearings

H. Toopchi-Nezhad*

Department of Civil Engineering, Razi University, Kermanshah, 67149-67346, Iran

(Received December 17, 2012, Revised December 12, 2013, Accepted December 27, 2013)

Abstract. Fiber Reinforced Elastomeric Bearings (FREBs) are a relatively new type of laminated bearings that can be used as seismic/vibration isolators or bridge bearings. In an unbonded (U)-FREB, the bearing is placed between the top and bottom supports with no bonding or fastening provided at its contact surfaces. Under shear loads the top and bottom faces of a U-FREB roll off the contact supports and the bearing exhibits rollover deformation. As a result of rollover deformation, the horizontal response characteristics of U-FREBs are significantly different than conventional elastomeric bearings that are employed in bonded application. Current literature lacks an efficient analytical horizontal stiffness solution for this type of bearings. This paper presents two simplified analytical models for horizontal stiffness evaluation of U-FREBs. Both models assume that the resistance to shear loads is only provided by an effective region of the bearing that sustains significant shear strains. The presented models are different in the way they relate this effective region to the horizontal bearing displacements. In comparison with experimental results and finite element analyses, the analytical models that are presented in this paper are found to be sufficiently accurate to be used in the preliminary design of U-FREBs.

Keywords: fiber reinforced elastomeric bearing; preliminary design; horizontal stiffness; seismic isolator; vibration isolator; bridge bearing; unbonded application

1. Introduction

Elastomeric bearings are used extensively in a variety of Structural and Mechanical Engineering Applications where a flexible structural support and/or vibration isolation is required. Typical applications for these bearings include, but not limited to, bridge bearings and vibration/seismic isolators. The main expectation from the bearing in these applications is to carry vertical loads with a minimum of deflection, and to allow horizontal and rotational movements with a minimal resistance.

Elastomeric bearings typically comprise alternating bonded layers of elastomer (rubber) and reinforcement materials such as steel plates or fiber fabric sheets. The elastomer layers provide horizontal and rotational flexibility, and the reinforcement layers provide vertical bearing stiffness by constraining the lateral bulging of the elastomer layers when the bearing is subjected to vertical compressive loads. Although Steel Reinforced Elastomeric Bearings (SREBs) are still the most

*Corresponding author, Assistant Professor, E-mail: h.toopchinezhad@razi.ac.ir; toopchi@gmail.com

Copyright © 2014 Techno-Press, Ltd.
http://www.techno-press.org/?journal=sem&subpage=8 ISSN: 1225-4568 (Print), 1598-6217 (Online)

common type of bearings, many research studies have shown that Fiber Reinforced Elastomeric Bearings (FREBs) are a viable alternative for conventional SREBs (Kelly 2002, Toopchi-Nezhad *et al.* 2008, 2009, Mordini and Strauss 2008, Dehghani Ashksari *et al.* 2008, and Khanlari *et al.* 2010).

Fiber reinforced bearings can be classified as *bonded* or *unbonded* bearings depending on their application. In a bonded (B)-FREB two thick steel mounting plates that are previously bonded to the top and bottom surfaces of the bearing are bolted to the top and bottom supports, respectively. In an unbonded (U)-FREB, no bonding or fastening is provided between the bearing and its top and bottom supports. As such, the shear loads at the bearing contact surfaces are transferred through friction only. As a result of unbonded boundary conditions, the horizontal response characteristic of a U-FREB becomes more complex and quite different than its B-FREI counterpart (Toopchi-Nezhad *et al.* 2011). A U-FREB exhibits rollover deformation under horizontal loads (see Fig. 1). As such, the closed form equations available for the horizontal stiffness evaluation of B-FREBs (Tsai and Kelly 2005a, b) are not applicable to U-FREBs. Current literature lacks an efficient analytical method that can be used in horizontal stiffness evaluation of U-FREBs. To address this lack, the focus of this study is on the horizontal stiffness evaluation of U-FREBs for preliminary design purposes.

Finite element analysis, as a powerful tool, has been employed in the horizontal stiffness evaluation of unbonded elastomeric bearings that exhibit rollover deformation (Kelly and Konstantinidis 2007, Toopchi-Nezhad *et al.* 2011, 2012, Gerhaher *et al.* 2011, Mishra and Igarashi 2012). The finite element analysis of U-FREBs is challenging and complicated. Challenges arise from the incompressibility of rubber material, changes in the boundary conditions of the bearing as a result of rollover deformation, and excessive distortion of finite element mesh as the bearing deforms horizontally (Toopchi-Nezhad *et al.* 2011). To address these challenges, the utilized finite element mesh should be updated repeatedly consistent with the deformed geometry of the bearing during the analysis. This frequent remeshing adds significantly to the costs and challenges of the finite element analysis. Since it is difficult to thoroughly incorporate the complex behavior of elastomer in the analysis, in most cases a finite element analysis can best serve as a tool for the preliminary design of bearing isolators. As a mandate enforced by current seismic codes (e.g., ASCE/SEI 7-10, 2010), the final design properties of bearing isolators should be evaluated through experimental studies on the bearing prototypes.

Given the complex horizontal response of U-FREBs, the application of finite element analysis may significantly increase the costs of the preliminary design of these bearings. In contrast, the availability and usage of a sufficiently accurate and easy to apply analytical model will significantly reduce these costs. Reducing the preliminary design costs is essential to the promotion of U-FREBs in many applications. This paper introduces two simple analytical models that can be used to approximate the horizontal stiffness of U-FREBs with sufficient accuracy. These models aim at evaluating the secant horizontal stiffness based on the overall bearing geometry, shear modulus of the rubber material, and the level of horizontal displacement imposed on the bearing. The main objective is to provide a useful tool for the preliminary design of U-FREBs.

2. The performance of elastomeric bearings: an overview

Steel Reinforced Elastomeric Bearings (SREBs) employ steel plates as the reinforcing material

to provide vertical bearing stiffness. In a horizontally deformed SREB shear is the dominant mode of deformation in the elastomer layers as the steel reinforcing plates remain relatively rigid in both extension and flexure. If the vertical load that is carried by the bearing is significantly lower than its buckling load, the secant horizontal stiffness, *K*, can be calculated using the following well known equation (Kelly 2007).

$$K = \frac{GA}{t_r} \tag{1}$$

where, *G* is the shear modulus of rubber, *A* is the plan area of the bearing, and t_r represents the total thickness of rubber layers in the bearing.

In Fiber Reinforced Elastomeric Bearings (FREBs) fiber fabric sheets are replaced with steel reinforcing plates to provide the vertical stiffness. In general, FREBs are relatively more flexible than SREBs for movements in the horizontal direction (Kelly 2002). This is due to the inplane flexibility and lack of flexural rigidity of fiber reinforcement sheets in FREBs. Unlike the steel reinforcing plates which remain nearly rigid in a horizontally deformed SREB, in a FREB the fiber reinforcement sheets exhibit warping deformations at their ends as the bearing deforms horizontally. Tsai and Kelly (2005a, b) developed a stiffness solution that accounts for the inplane flexibility and warping deformations of the fiber reinforcement sheets in B-FREBs. Overall, the stiffness solution presented by these researchers provides a more accurate estimation for the horizontal stiffness of B-FREBs as compared with Eq. (1). However, in many practical cases Eq. (1) may still be reasonably employed in the preliminary design of B-FREBs (Toopchi-Nezhad *et al.* 2011).

In a U-FREB the top and bottom surfaces of the bearing are not bonded to the contact supports. Therefore, under shear loads the bearing is held in place by friction. When the bearing is deformed horizontally, its top and bottom faces roll off the contact supports as a result of its unbonded boundary conditions (see Fig. 1). This at first sight might seem to be a deficiency, but it has the advantage that the horizontal bearing stiffness and the level of shear that is transmitted to the bearing supports are decreased with increasing horizontal displacements. As another advantage, the unbonded application eliminates the presence of tensile stresses in the bearing. The geometry of a U-FREB can be selected such that it maintains a positive incremental load-resisting capacity throughout its permissible range of horizontal displacements. The rollover deformation in such bearing is termed as "stable rollover" deformation (Toopchi-Nezhad *et al.* 2008).

The horizontal load-displacement relationship in a U-FREB is nonlinear as a result of rollover deformation. Accordingly, Eq. (1) that constructs a linear relationship between horizontal loads and displacements is not applicable to U-FREBs. Eq. (1) in its original form will largely overestimate the horizontal stiffness of U-FREBs (Toopchi-Nezhad *et al.* 2008).

3. Horizontal stiffness of U-FREBs

Fig. 1(a) contains a sketch of a U-FREB located between two horizontal rigid contact supports. When a horizontal displacement δ is imposed, the bearing exhibits rollover deformation due to its unbonded application (see Fig. 1(b)). A comparison between Figs. 1(a) and (b) indicates that the contact area between the bearing and its supports decreases with increasing horizontal bearing displacement. In other words, the boundary conditions of the bearing vary with displacements. The full-contact displacement, δ_{fc}, in a U-FREB is achieved when the originally vertical edges of the bearing completely contact the horizontal supports (Fig. 1(c)).

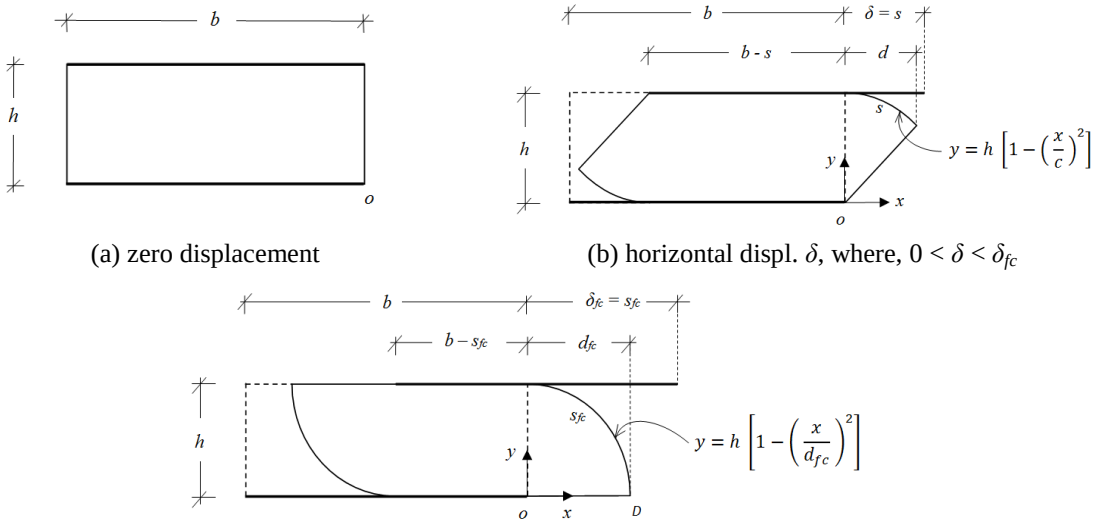

(a) zero displacement

(b) horizontal displ. δ, where, $0 < \delta < \delta_{fc}$

(c) full contact horizontal displacement, δ_{fc}

Fig. 1 A U-FREB under different horizontal displacements

As stated earlier in this paper, in many cases Eq. (1) can be used with sufficient accuracy for the preliminary design of B-FREBs. The most important aspects of a horizontally deformed B-FREB are that the boundary conditions of the bearing remain unchanged regardless horizontal displacements, and the profile of shear strain within the bearing remains approximately uniform (Toopchi-Nezhad *et al.* 2011). Since shear is the dominant mode of deformation in the entire bearing, the bearing plan area, A, can be employed in Eq. (1) to evaluate the horizontal stiffness. In a horizontally deformed U-FREB, however, the boundary conditions are changed with displacements. The uniform shear strains are only found at the central region of the bearing that is limited to the overlap region between its top and bottom surfaces. The shear strain decreases significantly at the bearing rollover regions (i.e., the regions that roll-off the contact supports when the bearing undergoes horizontal displacements). In analogy to Eq. (1), an effective plan area, A_{eff}, over which shear is the dominant mode of deformation may be used to approximate the horizontal stiffness, K, of a U-FREB. This leads to the following equation.

$$K = \frac{GA_{eff}}{t_r} \tag{2}$$

The effective plan area (A_{eff}) in a U-FREB will depend on the horizontal bearing displacements δ. At zero horizontal displacements, A_{eff} is equal to the original plan area, A, of the bearing. However, the influence of horizontal displacements is to decrease A_{eff}. Using Eq. (2) to evaluate the secant horizontal stiffness K of a U-FREB, the problem is reduced to constructing a relationship between δ and A_{eff}.

4. Bounds to the effective plan area, A_{eff}

It can be assumed that in a horizontally deformed U-FREB the free surface of the bearing's

rollover region remains stress free. Therefore, the length of the curved arc of the free surface (i.e., *s* in Fig. 1(b)) will be equal to the horizontal displacement δ that is imposed on the bearing. The lower bound to the effective plan area, A_{eff}, in a deformed U-FREB is the physical net contact area (A_{net}) between the bearing and its top or bottom support. This is given by

$$A_{lb} = A_{net} = a(b - \delta) \tag{3}$$

where, A_{lb} represents the lower bound plan area under horizontal displacement δ, and a and b are the width (out of plane dimension) and length (inplane dimension, in the horizontal direction) of the bearing, respectively.

The use of $A_{eff} = A_{net}$ in Eq. (2) results in an underestimate approximation of the horizontal stiffness as the contribution of the bearing rollover region in the horizontal stiffness is completely ignored. A previous finite element study (Toopchi-Nezhad *et al.* 2011) indicates that the profile of shear strain in the rollover region of a U-FREB decreases dramatically from its peak value at the bearing central region, to significantly smaller values (or even negative values at relatively large horizontal displacements) at regions close to the ends of the bearing. Therefore, as a more reasonable estimation for A_{eff}, the portion of the bearing rollover region that sustains significant shear strains should be taken into consideration.

Eq. (4) presents an effective plan area that accounts for the half of the rollover region of bearing. Due to the rapid rate of reduction of shear strain in the rollover region (Toopchi-Nezhad *et al.* 2011), shear strains are significant in only a small portion of this region. Therefore, the effective plan area given by Eq. (4) that accounts for 50% of the curved surface of the rollover region in addition to the net contact area, may be considered as an upper bound limit, A_{ub}, to A_{eff}. The use of A_{ub} in Eq. (2) is expected to result in an overestimate approximation of the bearing horizontal stiffness.

$$\mathrm{A_{ub}} = a\left(b - \frac{\delta}{2}\right) \tag{4}$$

Figs. 2(a) and (b) compare the experimentally obtained horizontal load-displacement hysteresis loops of two individual bearings, namely Bearings 1 and 2, with the load-displacement curves evaluated using the "underestimate" and "overestimate" models given by Eqs. (3) and (4), respectively. The physical and material properties of Bearings 1 and 2 can be found in Table 1. The experimental hysteresis loops of these bearings were evaluated through a set of cyclic testing during which the fully reversed cycles of horizontal displacements were applied while the bearings were subjected to a constant vertical pressure of 1.6 MPa. Since the analytical solutions presented in this paper are monotonic, only half of the experimental hysteresis loops are shown in Fig. 2. The underestimate-model in Fig. 2 uses A_{lb} to evaluate the horizontal stiffness. In the overestimate-model, A_{ub} is employed to evaluate the horizontal stiffness of the bearings. Having horizontal secant stiffness, K, calculated from Eq. (2) for any given δ, the shear load, F, is then evaluated by multiplying K by δ.

Figs. 2(a) and (b) show the normalized shear load F/GA (where, G and A are the shear modulus of the elastomer and the original plan area of the bearing, respectively) versus the normalized horizontal displacement δ/h (where, h is the total thickness of the bearing). As seen in these figures, the "underestimate" and "overestimate" models bracket the experimentally evaluated hysteresis loops of the bearings.

An examination of the hysteresis loops of Bearing 1 in Fig. 2(a) indicates that the horizontal response of this bearing is unstable. This is due to the negative horizontal tangent stiffness values

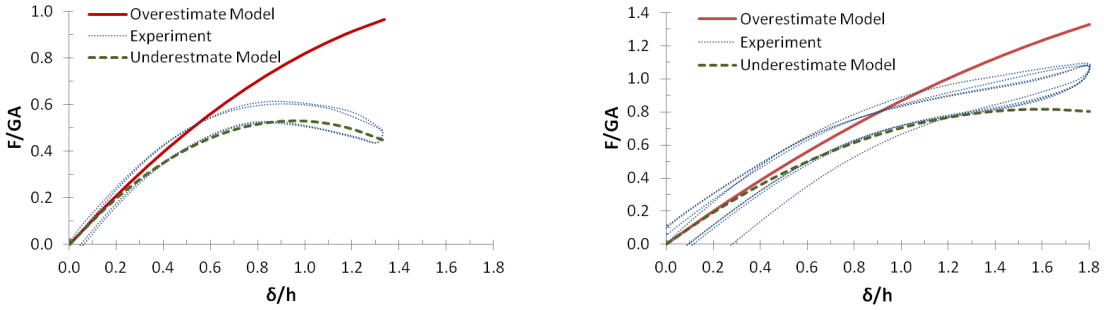

(a) Bearing 1 (b) Bearing 2

Fig. 2 Comparison between experimental results (Toopchi-Nezhad *et al.* 2008) and the analytical models that bracket the horizontal response

Table 1 Physical and material properties of benchmark U-FREBs

Bearing	1[a]	2[a]	3[b]	4[c]	5[c]	6[c]
Plan dimensions (a , b)	200	200	70	250	333	500
Height of the bearing (h)	105	69	25	100	100	100
Thickness of individual elastomer layers (t_e)	4.70	4.70	1.58	4.17	5.55	8.33
Number of elastomer layers (N_e)	20	12	12	24	18	12

Notes:
i. All dimensions are in mm
ii. Shear modulus of elastomer, G_e = 0.4 MPa in all of the bearings

[a] Ref.: Toopchi-Nezhad *et al.* (2008)
[b] Ref.: Toopchi-Nezhad *et al.* (2011)
[c] Ref.: Toopchi-Nezhad *et al.* (2012)

that occur at extreme bearing displacements. The overestimate-model is unable to capture the unstable load-deformation response of Bearing 1 as it maintains positive horizontal stiffness values throughout (see Fig. 2(a)). Even though the underestimate-model is able to simulate the unstable horizontal load-displacement behavior of Bearing 1, it underestimates the shear loads at horizontal displacements larger than approximately 0.2 h.

As seen in Fig. 2(b), the experimentally-evaluated horizontal response of Bearing 2 is stable. This is due to the fact that the horizontal tangent stiffness of this bearing remains positive throughout (see the hysteresis loops in Fig. 2(b)). The underestimate-model calculates zero and negative horizontal stiffness values for this bearing, which is not consistent with the experimental observations. For this bearing the overestimate-model significantly overrates the shear loads at horizontal displacements of approximately 0.6 h and above.

5. Analytical models to determine A_{eff}

As mentioned in the earlier section, in a horizontally deformed U-FREB the central region of bearing together with a small portion of its rollover region are subjected to significant shear strains only. To determine the effective plan area, A_{eff}, these regions are required to be reasonably taken

into account. The other requirement is that the value of A_{eff} be located between the bound limits given by Eqs. (3) and (4). In this section, two different analytical models that satisfy these requirements are developed to approximate A_{eff}. The two models developed in this paper are called hereafter as Model 1 and Model 2. The effectiveness of these models is investigated using previously conducted experimental studies and finite element analyses on a set of various U-FREBs.

The lower bound effective plan area that is given by Eq. (3) accounts for the central region of the bearing only. The upper bound effective plan area in Eq. (4) accounts for the central region and 50% of the rollover region of bearing. Model 1 simply takes the mean of these bound limits as the bearing effective plan area. This means that in Model 1 the contribution of 25% of the rollover region, in addition to the central region of bearing is taken into account in calculating the effective plan area, $A_{eff,1}$, as follows

$$A_{eff,1} = a\left(b - \tfrac{3}{4}\delta\right) \tag{5}$$

The effective plan area given by Eq. (5) is a function of the bearing plan dimensions a and b, and the level of horizontal bearing displacement, δ.

In the 2nd model, the effective plan area, $A_{eff,2}$, is calculated from Eq. (6), in which a new parameter denoted by d is deducted from the bearing length b to calculate $A_{eff,2}$. Parameter d physically represents the project of the curved arc of the rollover region along the horizontal axis (see Fig. 1(b)). As will be shown later on in this section, parameter d is a function of horizontal displacement δ, and the total thickness of bearing, h. According to Fig. 1(b), d is slightly smaller than δ (note that $\delta = s$). The term $a(b\text{-}d)$ in Eq. (6) can be expressed mathematically as $a[(b\text{-}s) + (s\text{-}d)]$, which means that the net contact area of $a(b\text{-}s)$ is extended by the amount of $a(s\text{-}d)$ to account for a small portion of the rollover region in calculating the bearing effective plan area $A_{eff,2}$.

$$A_{eff,2} = a(b - d) \tag{6}$$

The effective plan area in Eq. (6) in fact accounts for all of the bearing physical dimensions, namely, a, b, and h, together with the horizontal displacement δ. The influence of h and δ is embedded in parameter d. Since the value of $A_{eff,2}$ that is a function of parameters a, b, h, and δ is eventually substituted in Eq. (2), the horizontal bearing stiffness in Model 2 becomes a function of these parameters in conjunction with the total thickness of elastomer layers in the bearing, t_r, and the nominal shear modulus of the elastomer, G. Additionally, due to the presence of both h and t_r in the analysis, the influences of the thickness of fiber reinforcement layers, t_f, and the number of elastomer layers in the bearing, n, are taken into account implicitly as $h = t_r + (n\text{-}1)t_f$.

The deformed geometry shown in Fig. 1(b) is assumed in order to evaluate the value of d in a horizontally deformed U-FREB. This deformed geometry can also be used to estimate the ultimate horizontal bearing displacement (i.e., δ_{fc} in Fig. 1(c)) that is an essential parameter in the design of any U-FREB. As shown in Fig. 1(b), the curved free surface of the bearing rollover region can be simulated with a parabolic arc. The equation of this arc in the coordinate system x, y shown in Fig. 1(b), is

$$y = h\left[1 - \left(\frac{x}{c}\right)^2\right] \tag{7}$$

where, h is the total thickness of bearing and c is a constant.

It is assumed that the location of the origin of the coordinate x, y remains unchanged regardless the horizontal bearing displacements. This assumption is consistent with previous experimental

observations (e.g., Toopchi-Nezhad *et al.* 2008 and 2009). The constant c in Eq. (7) is determined to be equal to d_{fc} when the coordinate of point D in Fig. 1(c) is substituted in Eq. (7). As seen in Fig. 1(c), d_{fc} is the project of the curved arc along axis x at horizontal displacement δ_{fc}. Since d_{fc} is the ultimate value of d, it can be expressed as a function of the bearing geometry. In order to evaluate d_{fc}, it is essential to evaluate the length of the curved arc of the rollover region at full contact horizontal displacement, namely, s_{fc}. The length s of the curved arc at any horizontal displacement is calculated as follows

$$s = \int_0^d \sqrt{1 + \left(dy/dx\right)^2}\, dx \tag{8}$$

where, from Eq. (7) with $c = d_{fc}$

$$dy/dx = \frac{-2hx}{d_{fc}^2} \tag{9}$$

At full contact horizontal displacement shown in Fig. 1(c), the length of the curved arc is given by

$$s_{fc} = \int_0^{d_{fc}} \sqrt{1 + \left(\frac{-2hx}{d_{fc}^2}\right)^2}\, dx \tag{10}$$

The result of performing this integral is

$$s_{fc} = \frac{h}{2}\left[\sqrt{4 + \alpha_{fc}^2} + \frac{\alpha_{fc}^2}{2}\, ln\left(\frac{2+\sqrt{4+\alpha_{fc}^2}}{\alpha_{fc}}\right)\right] \tag{11}$$

where

$$\alpha_{fc} = \frac{d_{fc}}{h} \tag{12}$$

It is assumed that the elastomer material in the bearing is incompressible. Accordingly, the volume of bearing does not change with horizontal displacements. At full contact displacement (Fig. 1c), the area of the rollover region, $A_{rr,fc}$, that is enclosed by the curved arc of length s_{fc} is evaluated as follows

$$A_{rr,fc} = \int_0^{d_{fc}} y\, dx = \int_0^{d_{fc}} h\left[1 - \left(\frac{x}{d_{fc}}\right)^2\right] dx \tag{13}$$

Taking this integration, Eq. (13) leads to

$$A_{rr,fc} = \tfrac{2}{3}\alpha_{fc} h^2 \tag{14}$$

The constraint of incompressibility requires that the volume of bearing before and after deformation be the same, therefore

$$bh = \left(b - s_{fc}\right)h + 2A_{rr,fc} \tag{15}$$

From Eqs. (11), (14), and (15) α_{fc} is evaluated as

$$\alpha_{fc} = 1.25 \tag{16}$$

Using Eqs. (12) and (16), the constant $c = d_{fc}$ in Eq. (7) is evaluated as

$$c = d_{fc} = 1.25\, h \tag{17}$$

Substitute Eq. (16) in Eq. (11), and note that $s_{fc} = \delta_{fc}$, the full contact horizontal displacement, δ_{fc}, is calculated as

$$\gamma_{fc} = \frac{\delta_{fc}}{h} = 1.667 \cong 1.67 \tag{18}$$

where, γ_{fc} represents the nominal shear strain in the bearing at full contact horizontal displacement.

From Eqs. (17) and (18) d_{fc} is calculated to be approximately $0.748\, \delta_{fc}$. Substitute this value in Eq. (6), the bearing effective plan area at full contact horizontal displacement, $A_{eff,2,fc}$, is calculated as

$$A_{eff,2,fc} = a\left(b - 0.748\, \delta_{fc}\right) \tag{19}$$

A comparison between Eqs. (19) and (5) indicates that the coefficient of 0.748 in Eq. (19) of Model 2 is very close to the constant coefficient of ¾ that is used in Eq. (5) of Model 1. Therefore, at full contact horizontal displacement the results of Models 1 and 2 are expected to be in an excellent agreement.

At horizontal displacements smaller than δ_{fc}, the length of the curved arc of the rollover region, s, is calculated using Eq. (10) in which d_{fc} is replaced with d at the upper limit of the integral. This, results in

$$s = \int_0^d \sqrt{1 + \left(\frac{-2hx}{d_{fc}^2}\right)^2}\, dx \tag{20}$$

where, d_{fc} is given by Eq. (17). The closed form solution of the integral in Eq. (20) is

$$s = \tfrac{25}{64}\, h\left[2\beta\sqrt{1 + 4\beta^2} + ln\left(2\beta + \sqrt{1 + 4\beta^2}\right)\right] \tag{21}$$

where

$$\beta = \tfrac{16}{25}\,\alpha = \tfrac{16}{25}\left(\frac{d}{h}\right) \tag{22}$$

The following step by step procedure is followed in Model 2 to evaluate the horizontal stiffness and shear load in a U-FREB for a given level of horizontal displacement, δ.

1. let $s = \delta$
2. use a numerical technique solve Eq. (21) for β
3. from Eq. (22) calculate $d = \frac{25}{16}\,\beta h$
4. from Eq. (6) calculate $A_{eff} = a(b - d)$
5. use Eq. (2) calculate horizontal stiffness $K = \frac{GA_{eff}}{t_r}$
6. calculate horizontal load F (shear load) from $F = K\delta$

Notes:

i. In Model 1, steps 2 and 3 are ignored, and d in Step 4 is taken as $\frac{3}{4}\,\delta$

ii. Models 1 and 2 are valid for horizontal displacements up to the full contact displacement of

$\delta_{fc} \cong 1.67h$ that is given by Eq. (18)

6. Condition to achieve stable rollover deformation

A properly designed U-FREI must remain stable throughout its permissible range of horizontal displacements by maintaining a positive incremental load-displacement capacity. As such, in a U-FREI bearing that sustains a rollover deformation of δ, a horizontally-stable response is achieved if $dF/d\delta > 0$. Using Model 1, this condition is expressed as follows

$$\frac{dF}{d\delta} = \frac{d}{d\delta}\left(\frac{Ga\left(b-\frac{3}{4}\delta\right)\delta}{t_r}\right) > 0 \;\rightarrow\; b > \frac{3}{2}\delta \;\; or \;\; \delta < \frac{2}{3}b \tag{23}$$

Therefore, in a U-FREI bearing with given physical dimensions, the rollover deformation of the bearing remains stable as far as $\delta < \frac{2}{3}b$. On the other hand, a U-FREI bearing is expected to exhibit stable rollover until an extreme deformation of $\delta_{fc} = 1.67\,h$ (see Eq. (18)), if $b > \frac{3}{2}\delta_{fc}$, which means, if $b > 2.5\,h$. The latter condition may be used as a geometrical constraint in the preliminary design of U-FREI bearings.

7. Examination of models

Table 1 contains the physical and material properties of 6 different benchmark U-FREBs that are denoted by Bearings 1 to 6. The horizontal response characteristics of these bearings are investigated in previous research studies (Toopchi-Nezhad *et al.* 2008, 2011, 2013). The effectiveness of Models 1 and 2 in approximating the horizontal stiffness and simulating the load-displacement curves of these bearings is investigated in this section.

Figs. 3(a) and (b) contain the analytical load-displacement curves of Bearings 1 and 2, respectively, that are plotted on their experimental load-displacement hysteresis loops. Bearing 1 in Fig. 3(a) is a special bearing with unaccepted performance due to its horizontal instability. In practice, the designer would revise the details of such bearing to achieve a stable horizontal response before the preliminary design is complete. As such, it is critical for an acceptable analytical model to be able to predict the unstable horizontal response of this bearing in the preliminary design stage. According to Fig. 3(a) both Models 1 and 2 are able to capture the unstable behavior of the bearing as the horizontal tangent stiffness values in both curves approach zero at displacements below the full contact displacement. In both models, however, the zero tangent stiffness occurs at relatively larger horizontal displacements as compared to the experimental loops.

Fig. 3(b) compares the analytical load-displacement curves and the experimental hysteresis loops of Bearing 2. Unlike Bearing 1, Bearing 2 maintains a positive incremental load-displacement capacity throughout the range of horizontal displacements shown in Fig. 3(b). Therefore, it represents an acceptable response behavior as it remains stable horizontally. A reasonable simulation of the horizontal load-displacement curve of such bearing is deemed as an essential step in the preliminary design. As seen in Fig. 3(b), the load-displacement curves of Models 1 and 2 are reasonably consistent with the experimental hysteresis loops of Bearing 2. Accordingly, the horizontal stiffness values that are approximated by these models at different displacements are expected to be sufficiently accurate to carry out the preliminary design.

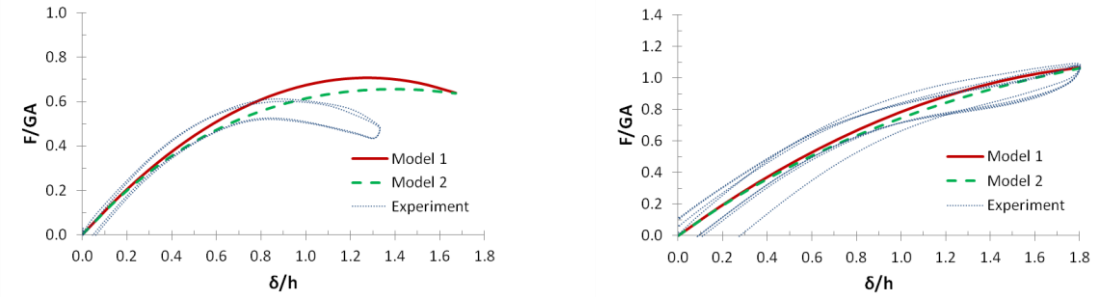

(a) Bearing 1 (b) Bearing 2

Fig. 3 Comparison between analytical models and experimental results

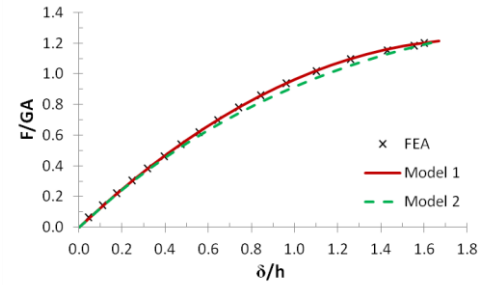

Fig. 4 Comparison between analytical models and finite element analysis for Bearing 3

An inspection of Figs. 3(a) and (b) reveals that the load-displacement curves in Models 1 and 2 approach to each other at the extreme horizontal bearing displacement. This is due to the fact that according to Eq. (19) at the extreme level of horizontal displacement (i.e., at δ_{fc}), d in Model 2 (see Eq. (6)) approaches to 3/4 δ that is employed by Model 1 (see Eq. (5)).

To further examine the effectiveness of Models 1 and 2, the horizontal bearing stiffness and the load-displacement curves of Bearings 3 to 6, cited in Table 1, are compared with the results of finite element analysis. These comparisons are reflected in Tables 2 and 3, and Figs. 4 and 5.

The analytical load-displacement curves of Bearing 3 that are predicted by Models 1 and 2 are shown in Fig. 4. This figure also contains the load-displacement curve of the bearing resulted by finite element analysis. In the finite element analysis, an incrementally increasing monotonic shear load was applied on the bearing while it was subjected to a constant vertical compression of 1.6 MPa. Detailed information on the finite element model of this bearing can be found in Ref. 6.

According to Fig. 4, there is an excellent agreement between the horizontal load-displacement curve predicted by Model 1 and that of the finite element analysis. Model 2 also shows a good correlation with the finite element results. However, as compared with the finite element analysis, Model 2 slightly underestimates the shear load at intermediate horizontal bearing displacements. Table 2 lists the analytically evaluated horizontal secant stiffness values of Bearing 3 at different displacements. It also contains the stiffness values calculated by the finite element analysis. As seen in this table, there is an excellent agreement between the results of Model 1 and the finite element analysis. A good correlation also exists between the results of Model 2 and the finite element analysis as the maximum error of approximately 5% in calculating the horizontal secant stiffness is achieved.

Table 2 Horizontal secant stiffness of Bearing 3 (comparison between the analytical models and FE-analysis)

Normalized horizontal displacement (δ/δ_{fc}[d])	FE-analysis	Model 1		Model 2	
	K (N/mm)	K (N/mm)	error %	K (N/mm)	error %
0.20	93.30	93.93	+0.67	91.32	-2.17
0.40	84.23	84.69	+0.55	80.71	-4.36
0.60	75.27	75.46	+0.25	71.68	-5.02
0.80	65.72	66.23	+0.77	63.85	-2.93
0.96	58.76	58.83	+0.12	58.26	-0.86

[d] δ_{fc} = 41.75 mm

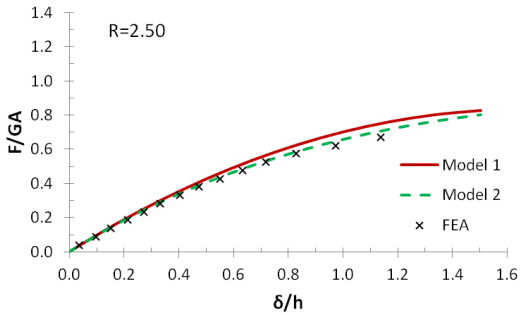

(a) Bearing 4

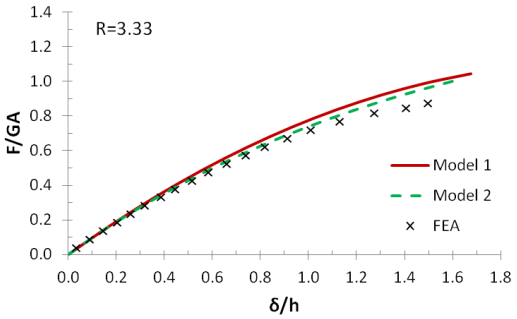

(b) Bearing 5

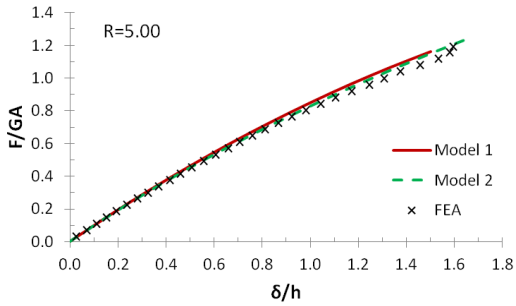

(c) Bearing 6

Fig. 5 Comparison between analytical models and finite element analysis for Bearings 4 to 6 with different aspect ratios, R

Horizontal load-displacement curves of Bearings 4 to 6 are shown in Fig. 5. These bearings share the same shape factor, S, of approximately 15. Shape factor is defined as the ratio of plan area to perimeter bulge-free area of single elastomer layers in the bearing. Although the shape factor for Bearings 4 to 6 is identical, these bearings have different aspect ratios, R, ranging from 2.5 to 5. By definition, R represents the ratio of length (parallel to the direction of horizontal displacements) to thickness of the bearing. In the finite element model a zero physical thickness has been assigned to the fiber reinforcement layers of these bearings (Toopchi-Nezhad *et al.* 2013). Accordingly, the physical thickness of these bearings is limited to the total thickness of their elastomer layers, namely, 100 mm. To remain consistent with the finite element model, the thickness of the fiber reinforcement layers in the analytical models is taken zero. Therefore, for

Table 3 Accuracy of Models 1 and 2 with respect to the FEA in evaluating the horizontal secant stiffness of Bearings 4 to 6

Normalized horizontal displacement (δ/δ_{fc}[e])	Bearing 4 (X[f] = 0.76)			Bearing 5 (X[f] = 0.90)			Bearing 6 (X[f] = 0.96)		
	FEA K (N/mm)	Model 1 error %	Model 2 error %	FEA K (N/mm)	Model 1 error %	Model 2 error %	FEA K (N/mm)	Model 1 error %	Model 2 error %
0.2	212.72	+5.44	+2.12	387.95	+5.43	+3.14	925.04	+2.62	+1.08
0.4	186.19	+6.85	+1.28	352.39	+6.50	+2.73	866.94	+3.65	+1.22
0.6	158.15	+9.54	+3.66	316.55	+7.86	+3.98	812.74	+4.36	+1.93
0.8	N/A			278.07	+10.36	+7.76	758.61	+5.13	+3.53
X[f]	134.21	+13.08	+8.54	258.31	+11.96	+10.46	756.36	+0.33	-0.10

[e] δ_{fc} = 167 mm for all of the bearings cited in this table
[f] X indicates the maximum ratio of δ/δ_{fc} achieved in the FEA.

each of Bearings 4 to 6 the total thickness of elastomer layers, t_r, is the same as the total thickness of the bearing, h.

As seen in Fig. 5(a) for Bearing 4 of R = 2.50 Model 2 is in an excellent agreement with the finite element analysis. According to this figure, Model 1 slightly overestimates the shear loads at large bearing displacements. It should be noted that the finite element analysis for this bearing could not converge to a unique solution at displacements beyond 1.15 h. This was probably due to the fact that the horizontal tangent stiffness of the bearing acquired values close to zero at displacements greater than this limit (Toopchi-Nezhad *et al.* 2011). The accuracy of the analytical models with respect to the finite element results can be observed in Table 3. As seen in this table, the maximum absolute value of errors in evaluating the bearing horizontal secant stiffness is approximately 13% in Model 1, and nearly 8% in Model 2. In the load-displacement curve constructed by Model 1 the slope of the load-displacement curve, i.e., the tangent stiffness, remains marginally positive at the full contact displacement. This indicates that there is only a small margin of safety against horizontal instability with the aspect ratio of 2.5 for this bearing.

The horizontal load-displacement curves of Bearing 5 with R = 3.33 are shown in Fig. 5(b). According to this figure at low to intermediate displacements there is a good agreement between both of the analytical models and the finite element analysis. However, the accuracy of the analytical models diminishes with increasing bearing displacements (see Table 3). The maximum error resulted by Models 1 and 2 in evaluating the horizontal bearing stiffness are approximately 12% and 10.5%, respectively. Overall, the results of Model 2 for Bearing 5 are in a relatively better agreement with the finite element analysis results.

Fig. 5(c) shows the load-displacement curves of Bearing 6 resulted by the analytical models and the finite element analysis in which an excellent agreement between the latter analysis and the analytical models can be observed. Table 3 lists the resulting errors in the analytical estimation of secant horizontal stiffness at different displacements. As cited in this table, the maximum errors in the evaluation of stiffness in Models 1 and 2 are found to be 5% and 3.5%, respectively.

As seen in Figs. 3 to 5, the level of shear load at the intermediate to large horizontal displacements in Model 2 is relatively lower than in Model 1. Additionally, at small horizontal displacements as well as at full-contact horizontal displacement both models yield to approximately identical results. This indicates that the lower bound limit to parameter d in Eq. (6)

is ¾ δ. Note that this lower bound limit, i.e., ¾ δ is used in Model 1 (see Eq. (5)).

8. Limitations of models

The analytical models developed in this paper serve as a tool for the preliminary design of U-FREBs. Both models assume that the bearing is subjected to a relatively light vertical compressive load so that the influences of the vertical load and the vertical bearing deflection in the horizontal stiffness can be neglected. The 3D effects are neglected in both models. In both models the bearing is treated as a monolithic material with width, length, and height of a, b, and h, respectively. The total thickness of the elastomer layers, t_r, and the shear modulus of the elastomer material, G, are two additional parameters which are accounted for in calculating the secant horizontal stiffness of the bearing. Both models simulate the load-displacement response under monotonic lateral loads. They both utilize a nominal constant value for the shear modulus G. This value is assumed to be independent of the level of shear strain in the elastomer. As such, the stress-softening of the elastomer, which occurs under reversal cycles of loading and is known as Mullin's effect (Mullins 1969), is not addressed by the simplified models presented in this study.

The material property and inplane stiffness of fiber reinforcement layers are disregarded in the analysis by both models. Results of a previous research study (Toopchi-Nezhad *et al.* 2013) indicate that the properties of fiber reinforcement layers do primarily affect the vertical stiffness of a U-FREB. The horizontal stiffness is to some limited extend influenced by the inplane stiffness of fiber reinforcement layers.

Model 1 does not account for the thickness of individual elastomer layers, t_e, or individual fiber reinforcement layers, t_f, within the bearing. However, these parameters are embedded in t_r and h that are employed in Model 2 (note that d in Eq. (6) is a function of h). Nonetheless, an examination of Tables 2 and 3 indicates that the results of Models 1 and 2 for the bearings considered in this study are comparable. A previous study (Toopchi-Nezhad *et al.* 2013) suggests that in general the thickness of individual elastomer layers, t_e, is not a critical parameter in controlling the horizontal stiffness of a U-FREB. The horizontal stiffness is primarily influenced by the total thickness of elastomer layers, t_r.

9. Conclusions

This paper introduces two simplified analytical models which can be used in the preliminary horizontal stiffness evaluation of Unbonded-Fiber Reinforced Elastomeric Bearings (U-FREBs). Both models assume that at any given horizontal displacement, only an effective region of the bearing that sustains significant shear strain contributes in the horizontal stiffness. This effective region includes the central bearing region and a small portion of the rollover region of the bearing. The central region of a horizontally deformed bearing is the region that remains in contact with top and bottom supports. The rollover region is referred to the region that rolls off the contact support when the bearing is deformed horizontally. Since shear is assumed to be the dominant mode of deformation, the horizontal stiffness is evaluated using $K = GA_{eff}/t_r$. This equation is similar to the well-known equation that is widely used in the stiffness evaluation of conventional steel reinforced bearings. However, the bearing's plan area, A, that is used in the original equation has been replaced with an effective plan area, A_{eff}. The two models presented in this paper differ by the way

they evaluate A_{eff}.

In both models A_{eff} is expressed as a function of the bearing length, width, and the level of horizontal displacement imposed on the bearing. Model 1 neglects the thickness of individual elastomer and fiber reinforcement layers within the bearing. However, Model 2 accounts for these parameters implicitly by including the total thickness of the bearing in the analysis. The effectiveness of the models is investigated through comparing their evaluated horizontal stiffness and the experimental data as well as the results of finite element analysis. The maximum error in evaluating the horizontal stiffness values for the bearings investigated in this paper is found to be approximately 13% and 10% in Models 1 and 2, respectively. These error values suggest that both models in general are sufficiently accurate for the preliminary design purposes. In many practical cases the preliminary design may be carried out by implementing either of the models developed in this paper. However, for critical applications one may incorporate both of these models in the analysis and carry out the preliminary design based on the most critical analysis results.

Achieving horizontal stability is an important design requirement for U-FREBs. In a horizontally-stable U-FREB the slope of horizontal load-displacement curve remains positive throughout the permissible range of horizontal bearing displacements. Since the load-displacement curve of the bearing can be constructed in both models, the models are capable of examining the horizontal stability of U-FREBs. The extreme bearing displacement is achieved when the originally vertical faces of the bearing come in complete contact with the top and bottom supports. This extreme level of displacement, also called the full contact horizontal displacement, is found to be approximately 1.67 times the total thickness of the bearing, h.

The essential steps in the preliminary design of a U-FREB include, but not limited to: i) estimation of the full contact horizontal displacement of the bearing to ensure that it will satisfy the displacement demand; ii) evaluation of the horizontal secant stiffness of the bearing at any given displacement in order to construct the horizontal load-displacement curve and verify if the bearing is sufficiently flexible to meet the design objectives; and iii) verification of the bearing horizontal stability by examining the slope of the load-displacement curve throughout the entire range of bearing displacements. These essential preliminary design steps are successfully addressed by the simplified analytical models presented in this paper.

References

ASCE/SEI 7-10 (2010), *Minimum Design Loads for Buildings and Other Structures*, American Society of Civil Engineers, Reston, Virginia.

Dehghani Ashkezaria, G., Aghakouchak, A.A. and Kokabib, M. (2008), "Design, manufacturing and evaluation of the performance of steel like fiber reinforced elastomeric seismic isolators", *J. Mater. Process. Tech.*, **197**, 140-150.

Gerhaher, U., Strauss, A. and Bergmeister, K. (2011), "Numerical modeling of elastomeric bearings in structural engineering", *Adv. Mater. Sci*., **3**(29), 51-63.

Kelly, J.M. (2002), "Seismic isolation systems for developing countries", *Earthq. Spectra*, **18**(3), 385–406.

Kelly, J.M. and Konstantinidis, D. (2007), "Low-cost seismic isolators for housing in highly-seismic developing countries", *Proceedings of 10th World Conference on Seismic Isolation, Energy Dissipation and Active Vibrations Control of Structures*, Istanbul, Turkey.

Kelly, J.M. (2007), *Earthquake-Resistant Design with Rubber*, 2nd Edition, Springer, London.

Khanlari, S., Dehghani Ashkezari, G., Kokabi, M. and Razzaghi Kashani, M. (2010), "Fiber-reinforced nanocomposite seismic isolators: design and manufacturing", *Polymer Compos*., **31**(2), 299-306.

Mishra, H.K. and Igarashi, A. (2012), "Experimental and analytical study of scrap tire rubber pad for seismic isolation", *World Acad. S., Eng. and Technol.*, **62**, 202-208.
Mordini, A. and Strauss, A. (2008), "An innovative earthquake isolation system using fiber reinforced rubber bearings", *Eng. Struct.*, **30**(10), 2739-51.
Mullins, L. (1969), "Softening of rubber by deformation", *Rubber Chem. Technol.*, **42**, 339-62.
Toopchi-Nezhad, H., Tait, M.J. and Drysdale, R.G. (2008), "Testing and modeling of square carbon fiber-reinforced elastomeric seismic isolators", *Struct. Contrl. Health Monit.*, **15**(6), 876-900.
Toopchi-Nezhad, H., Tait, M.J. and Drysdale, R.G. (2009), "Shake table study on an ordinary low-rise building seismically isolated with SU-FREIs (stable unbonded fiber-reinforced elastomeric isolators)", *Earthq. Eng. Struct. Dyn.*, **38**(11), 1335-57.
Toopchi-Nezhad, H., Tait, M.J. and Drysdale, R.G. (2011), "Bonded versus unbonded strip fiber reinforced elastomeric isolators: finite element analysis", *Compos. Struct.*, **93**, 850-859.
Toopchi-Nezhad, H., Tait, M.J., and Drysdale, R.G. (2013), "Influence of thickness of individual elastomer layers (1st shape factor) on the response of unbonded fiber reinforced elastomeric bearings", *J. Compos. Mater.*, **47**(27), 3433-3450.
Tsai, H.C. and Kelly, J.M. (2005a), "Buckling of short beams with warping effect included", *Int. J. Solids Struct.*, **42**(1), 239-53.
Tsai, H.C. and Kelly, J.M. (2005b), "Buckling load of seismic isolators affected by flexibility of reinforcement" *Int. J. Solids Struct.*, **42**(1), 255-69.